square-voltammetry measurements a Princeton Applied Research (PAR) Model 273 potentiostat galvonastat was used interfaced to a Hewlett-Packard 9816 computer. Square-wave voltammetry measurements were made at a frequency of 5 kHz with a step height of 5 mV, and square-wave amplitude of 50 mV. A commercially available Pt electrode (Bioanalytical Systems), 10 μm in diameter, was used as a working electrode. A Pt wire or gauze constituted the counter electrode. The oxidation potentials (E^{ox}_D) given in the Tables II-IV correspond to the peak potentials obtained from the square-wave voltammetry experiments. These peak potentials are equivalent to $E^{\circ\prime}$ for reversible redox couples. The reference redox couple ferrocene/ferrocenium established the reference potential. The potentials were normalized to the SCE electrode by the addition of 0.44 V. The oxidation potential of the 4,4'-dimethoxystilbene (DMS) monitor obtained in acetonitrile by this method is 1.07 V vs SCE. The oxidation potentials of the tritolylamine (TTA) and trianisylamine (TAA) monitors are 0.75 and 0.52 V vs SCE, respectively.[50b]

Acknowledgment. We thank R. E. Moody and B. Armitage for technical assistance, J. E. Eilers for help with the MO calculations, J. R. Lenhard for the spectroelectrochemical measurement and the reduction potentials of DCA and TCA, V. D. Parker (Trondheim, Norway) for measuring the oxidation potential of biphenyl, and F. D. Saeva and R. H. Young for helpful discussions.

Registry No. 1, 108-38-3; **2**, 95-47-6; **3**, 108-67-8; 4, 106-42-3; **5**, 95-63-6; 6, 488-23-3; **7**, 527-53-7; **8**, 14108-88-4; **9**, 95-93-2; **10**, 29966-04-9; **11**, 1079-71-6; **12**, 700-12-9; **13**, 87-85-4; **14**, 92-52-4; **15**, 612-75-9; **16**, 91-20-3; **17**, 86-73-7; **18**, 91-57-6; **19**, 613-33-2; **20**, 581-42-0; **21**, 85-01-8; **22**, 2531-84-2; **23**, 1576-67-6; DCA, 1217-45-4; TCA, 80721-78-4; DMS, 4705-34-4; TTA, 1159-53-1; TAA, 13050-56-1; $DCA^{\bullet-}$, 22027-33-4; $Ph_2^{\bullet+}$, 34507-30-7; p-$MeOC_6H_4CH{=}CHC_6H_4$-p-$OMe^{\bullet+}$, 63464-03-9; $(p\text{-}MeC_6H_4)_3N^{\bullet+}$, 34516-45-5; $(p\text{-}MeOC_6H_4)_3N^{\bullet+}$, 34516-46-6; p-$MeC_6H_4Me^{\bullet+}$, 34510-22-0; durene radical cation, 34473-49-9; naphthalene radical cation, 34512-27-1; phenanthrene radical cation, 34504-68-2.

Coadsorption of Ferrocene-Terminated and Unsubstituted Alkanethiols on Gold: Electroactive Self-Assembled Monolayers

Christopher E. D. Chidsey,* Carolyn R. Bertozzi, T. M. Putvinski, and A. M. Mujsce

Contribution from the AT&T Bell Laboratories, Murray Hill, New Jersey 07974.
Received December 4, 1989

Abstract: Self-assembled monolayers provide an ideal system for disentangling the fundamental events in interfacial electron transfer. Coadsorption of ferrocene-terminated alkanethiols with unsubstituted *n*-alkanethiols on evaporated gold films yields stable, electroactive self-assembled monolayers. Monolayers containing low concentrations of alkanethiols linked to ferrocene by a polar ester group ($FcCO_2(CH_2)_nSH$, Fc = $(\eta^5\text{-}C_5H_5)Fe(\eta^5\text{-}C_5H_4)$) show thermodynamically ideal surface electrochemistry in 1 M $HClO_4$, indicating the ferrocene groups to be homogeneous and noninteracting. Higher surface concentrations or use of alkanethiols linked directly to the nonpolar ferrocene group ($Fc(CH_2)_nSH$) lead to broadened electrochemical features, indicating interactions among ferrocene groups or inhomogeneous sites. Longer chain lengths and lower ferrocene surface concentrations result in slower electron-transfer kinetics with the ferrocene groups. A fraction of the thiols in a monolayer exchange with thiols in an ethanol solution, but much of the monolayer remains unequilibrated after 10 days. Concurrent with exchange of a fraction of the electroactive adsorbates for electroinactive ones, there is a substantial decrease in the rate of electron transfer with the remaining electroactive groups. We suggest lattice and domain-boundary models of the mixed monolayers, which qualitatively explain our results and which indicate that quantitative studies of electron-transfer kinetics in this system will be very fruitful.

Detailed understanding and rational control of electron-transfer events at the electrochemical interface require structural insight and structural control. The electronic coupling between an electrode and an electroactive molecular site remains poorly understood despite extensive studies of outer-sphere electrochemical kinetics[1-3] and of chemical modification of electrode surfaces.[4-13] In the most significant work to date on the relationship between interfacial structure and electronic coupling, Li and Weaver showed that the rate of the irreversible reduction of cobalt(III) to cobalt(II) decreased exponentially with the number of atoms in the bifunctional ligand linking the cobalt(III) center to a gold surface.[14] However, the structure of that interface was unknown beyond the bond connectivities. Here we report a chemistry for incorporating a reversible, outer-sphere redox couple into an

(1) (a) Phelps, D. K.; Kornyshev, A. A.; Weaver, M. J. *J. Phys. Chem.* **1990**, *94*, 1454-1463, and references therein. (b) McManis, G. E.; Golovin, M. N.; Weaver, M. J. *J. Phys. Chem.* **1986**, *90*, 6563-6570.
(2) Yoshimori, A.; Kakitani, T.; Mataga, N. *J. Phys. Chem.* **1989**, *93*, 3694-3702.
(3) Iwasita, T.; Schmickler, W.; Schultze, J. W. *Ber. Bunsenges. Phys. Chem.* **1985**, *89*, 138-142.
(4) Murray, R. W. In *Electroanalytical Chemical Vol. 13*; Bard, A. J., Ed.; Marcel Dekker: New York, 1984; pp 191-368 and references therein.
(5) Bunding Lee, K. A.; Mowry, R.; McLennan, G.; Finklea, H. O. *J. Electroanal. Chem.* **1988**, *246*, 217-224.
(6) Bravo, B. G.; Michelhaugh, S. L.; Soriaga, M. P. *J. Electroanal. Chem.* **1988**, *241*, 199-210.
(7) Diaz, A.; Kaifer, A. E. *J. Electroanal. Chem.* **1988**, *249*, 333-338.
(8) Hickman, J. J.; Zou, C.; Ofer, D.; Harvey, P. D.; Wrighton, M. S.; Laibinis, P. E.; Bain, C. D.; Whitesides, G. M. *J. Am. Chem. Soc.* **1989**, *111*, 7271-7272.
(9) Widrig, C. A.; Majda, M. *Langmuir* **1989**, *5*, 689-695.
(10) Zhang, X.; Bard, A. J. *J. Am. Chem. Soc.* **1989**, *111*, 8098-8105.
(11) Donohue, J. J.; Buttry, D. A. *Langmuir* **1989**, *5*, 671-678.
(12) Katz, E. Y.; Solov'ev, A. A. *J. Electroanal. Chem.* **1989**, *261*, 217-222.
(13) Ueyama, S.; Isoda, S.; Maeda, M. *J. Electroanal. Chem.* **1989**, *264*, 149-156.
(14) Li, T. T.-T.; Weaver, M. J. *J. Am. Chem. Soc.* **1984**, *106*, 6107-6108.

0002-7863/90/1512-4301$02.50/0

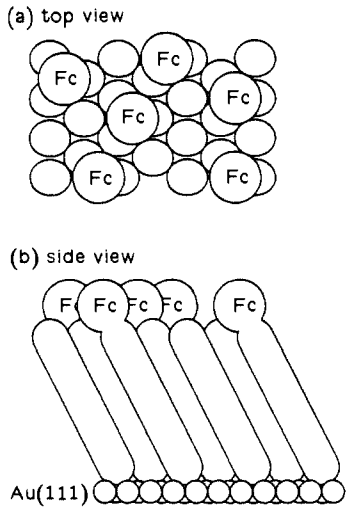

Figure 1. Model of a mixed monolayer containing ferrocene-terminated (Fc) and unsubstituted alkanethiols coadsorbed on the Au(111) surface. See text for structural details.

electrochemical interface at well-defined distances from an electrode. These assemblies will be valuable for exploring the role of structure in electron-transfer kinetics and as prototypes for more elaborate assemblies as the scope of preparative interfacial chemistry expands.

Our work builds on the growing body of knowledge of self-assembled monolayers.[15-31] The monolayer self-assembly technique is based on a judicious choice of both the adsorption chemistry and also the molecular shape of the adsorbate. By choosing an adsorption chemistry which is selective but stable, a large variety of functional groups can be incorporated into the adsorbed molecule without disrupting the expected connectivity with the substrate. By choosing an appropriate set of molecular shapes, dense crystalline-like packing can be achieved in a monomolecular layer. In favorable cases, one can hope for a unique and well-defined monolayer structure. To date, monolayer self-assembly chemistries include thiols,[16-25] disulfides[15,26] and sulfides[14,27] on gold; fatty acids on metal oxides;[28] silanes on silicon dioxide and alcohol surfaces;[29,30] phosphonates on metal phosphonate surfaces;[31] and isonitriles on platinum.[8] Many more are certainly possible. In the work reported here we use two different thiols, one of which is electroactive, coadsorbed onto gold surfaces to form electroactive, self-assembled monolayers that have a well-defined structure.

Figure 1 shows a lattice model of the type of monolayer assemblies we aim to prepare. Electroactive ferrocene groups (Fc = $(\eta^5\text{-}C_5H_5)Fe(\eta^5\text{-}C_5H_4)$), modeled as spheres with a diameter of 6.6 Å,[32,33] are connected to the electrode through alkanethiol chains, modeled as cylinders with a diameter of 4.6 Å.[23] The electroactive thiols are diluted with unsubstituted alkanethiols, also modeled as cylinders. The adsorbates are spaced 5.0 Å apart in a $\sqrt{3} \times \sqrt{3}$ R30° overlayer lattice on the gold(111) face.[22,24] The chains are tilted about 27° to achieve as dense packing as possible.[20,23] This model monolayer is thus a two-dimensional crystalline solution of electroactive and electroinactive adsorbates. It has two essential features. First, the unsubstituted alkanethiols keep the ferrocene groups well-separated from one another despite their relatively large size. This separation should ensure that their electrochemistry is that of identical, isolated sites. Second, the region of densely packed polymethylene chains keeps the ferrocene groups a well-defined and variable distance from the electrode surface. Varying the length of the chains should allow the distance dependence of the rate of electron transfer to be directly probed.

In previous attempts to use self-assembled monolayers to control electron transfer, investigators have used *n*-alkanethiols on gold to block electron transfer between an electrode and an electroactive species dissolved in an electrolyte solution.[16-18,23] The use of a Langmuir–Blodgett film has also been reported.[34] Although tremendous decreases in the average rate of interfacial electron transfer are observed, it is hard to rule out rapid electron transfer at a few defect sites as the dominant contribution to the measured electron-transfer current.[17,18,23] By replacing the freely diffusing electroactive species with covalently attached electroactive groups, we hope to achieve a significant advantage. The expected low mobilty of the densely packed hydrocarbon chains should limit the diffusion of the attached electroactive sites to defects. Electroactive sites not at defects will either exchange electrons with the electrode across the normal thickness of the monolayer (the desired pathway) or will exchange electrons with each other until the electrons diffuse to defects. This latter process can be probed by changing the concentration of electroactive sites in the monolayer. A second technical advantage of using covalently attached electroactive groups is that the reduction and oxidation currents will be transient currents, rather than the nearly steady-state currents obtained at monolayer-covered electrodes with electroactive species in solution. Kinetic heterogeneity among the sites should be readily identifiable from the time or frequency dependence of the transient currents.

In this paper, we lay the groundwork for future kinetic studies. We examine the electrochemical properties of monolayers of alkanethiols terminated with both polar and nonpolar ferrocene groups diluted with unsubstituted *n*-alkanethiols. The relative concentrations and the chain length of both the ferrocene-terminated and the unsubstituted thiols are varied. Exchange of ferrocene-terminated thiols for unsubstituted thiols proves to be useful both as a measure of defects and also as a way to avoid the influence of defects on the kinetics of electron transfer to the remaining ferrocene sites. This paper demonstrates that self-assembly will be a valuable tool for probing the role of distance and interfacial structure in interfacial electron transfer.

Experimental Section

Adsorbates. The *n*-alkanethiols are obtained from Aldrich and used without further purification. The ω-(ferrocenylcarbonyloxy)alkanethiols

(15) Nuzzo, R. G.; Allara, D. L. *J. Am. Chem. Soc.* **1983**, *105*, 4481–4483.
(16) Porter, M. D.; Bright, T. B.; Allara, D. L.; Chidsey, C. E. D. *J. Am. Chem. Soc.* **1987**, *109*, 3559–3568.
(17) (a) Finklea, H. O.; Avery, S.; Lynch, M.; Furtsch, T. *Langmuir* **1987**, *3*, 409–413. (b) Finklea, H. O.; Snider, D. A.; Fedyk, J. *Langmuir* **1990**, *6*, 371–376.
(18) (a) Sabatani, E.; Rubinstein, I.; Maoz, R.; Sagiv, J. *J. Electroanal. Chem.* **1987**, *219*, 365–371. (b) Sabatani, E.; Rubinstein, I. *J. Phys. Chem.* **1987**, *91*, 6663–6669. (c) Rubinstein, I.; Steinberg, S.; Tor, Y.; Shanzer, A.; Sagiv, J. *Nature* **1988**, *332*, 426–429.
(19) Bain, C. D.; Troughton, E. B.; Tao, Y.-T.; Evall, J.; Whitesides, G. M.; Nuzzo, R. G. *J. Am. Chem. Soc.* **1989**, *111*, 321–335.
(20) Nuzzo, R. G.; Dubois, L. H.; Allara, D. L. *J. Am. Chem. Soc.* **1990**, *112*, 558–569.
(21) Nuzzo, R. G.; Korenic, E. M.; Dubois, L. H. *J. Chem. Phys.* In press.
(22) Chidsey, C. E. D.; Liu, G.-Y.; Rowntree, P.; Scoles, G. *J. Chem. Phys.* **1989**, *91*, 4421–4423.
(23) Chidsey, C. E. D.; Loiacono, D. N. *Langmuir* **1990**, *6*, 682–691.
(24) Strong, L.; Whitesides, G. M. *Langmuir* **1988**, *4*, 546–558.
(25) (a) Bain, C. D.; Evall, J.; Whitesides, G. M. *J. Am. Chem. Soc.* **1989**, *111*, 7155–7164. (b) Bain, C. D.; Whitesides, G. M. *J. Am. Chem. Soc.* **1989**, *111*, 7164–7175.
(26) Bain, C. D.; Biebuyck, H. A.; Whitesides, G. M. *Langmuir* **1989**, *5*, 723–727.
(27) Troughton, E. B.; Bain, C. B.; Whitesides, G. M.; Nuzzo, R. G.; Allara, D. L.; Porter, M. D. *Langmuir* **1988**, *4*, 365–385.
(28) Allara, D. L.; Nuzzo, R. G. *Langmuir* **1985**, *1*, 45–52, and references therein.
(29) (a) Maoz, R.; Sagiv, J. *Langmuir* **1987**, *3*, 1034–1044. (b) Maoz, R.; Sagiv, J. *Langmuir* **1987**, *3*, 1045–1051. (c) Maoz, R.; Netzer, L.; Gun, J.; Sagiv, J. *J. Chim. Phys.* **1988**, *85*, 1059–1065.
(30) (a) Tilman, N.; Ulman, A.; Schildkraut, J. S.; Penner, T. L. *J. Am. Chem. Soc.* **1988**, *110*, 6136–6144. (b) Tillman, N.; Ulman, A.; Penner, T. L. *Langmuir* **1989**, *5*, 101–111.
(31) (a) Lee, H.; Kepley, L. J.; Hong, H.-G.; Akhter, S.; Mallouk, T. E. *J. Phys. Chem.* **1988**, *92*, 2597–2601. (b) Akhter, S.; Lee, H.; Hong, H.-G.; Mallouk, T. E.; White, J. M. *J. Vac. Sci. Technol. A* **1989**, *7*, 1608–1613.

(32) The size of the ferrocene group was estimated by determining the diameter of close-packed spheres that would have the crystallographic density of ferrocene.[33] An alternate approach, determining the diameter of close-packed spheres that would have the density of the most densely packed plane in the ferrocene crystal (110),[33] gave a slightly smaller value (6.4 Å).

(33) Seiler, P.; Dunitz, J. D. *Acta Crystallogr.* **1979**, *B35*, 1068–1074.

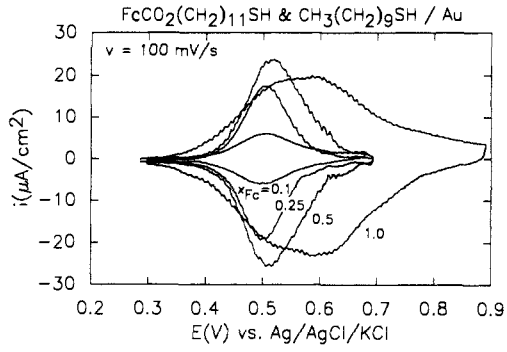

Figure 2. Cyclic voltammograms in 1 M $HClO_4$ of mixed monolayers of $FcCO_2(CH_2)_{11}SH$ and $CH_3(CH_2)_9SH$ formed from ethanol solutions containing various mole fractions (x_{Fc}) of the ferrocene-terminated thiol. Scan rate = 100 mV/s.

($FcCO_2(CH_2)_nSH$, Fc = $(\eta^5\text{-}C_5H_5)Fe(\eta^5\text{-}C_5H_4)$) are synthesized by the esterification of ferrocene carboxylic acid and an ω-bromoalkanol, conversion of the bromide to a thioacetate with sodium thioacetate, and, finally, mild hydrolysis of the thioacetate with sodium carbonate. The ω-ferrocenylalkanethiols ($Fc(CH_2)_nSH$) are synthesized by the acylation of ferrocene with an ω-bromoalkanoyl chloride, conversion of the terminal bromide group to a thioacetate, Clemmenson reduction of the ketone group, and finally acidic ethanolysis of the thioacetate group. The identity and purity of each adsorbate is confirmed by ^1H NMR spectroscopy, mass spectrometry, and elemental analysis. Synthetic and analytical details are provided in the Supplementary Materials.

Monolayer Preparation. The thiol monolayers are formed by soaking gold substrates in ethanol solutions of a ferrocene-terminated thiol and an unsubstituted thiol at 1 mM total thiol concentration. The mole fraction of ferrocene-terminated thiol in the solution to total thiol is denoted x_{Fc} and is varied from 0.0 to 1.0. The samples are removed from the adsorption solutions after a period of from 2 days to many weeks and washed sequentially with ethanol, hexane, ethanol, and finally water. No differences are observed for samples soaked for different periods of time. The substrates are freshly evaporated gold films on silicon wafers with adhesion layers of titanium. The gold crystallites in the films are of exclusively (111) crystallographic orientation. Full details of substrate preparation and characterization have been reported.[23]

Electrochemical Measurements. Electrochemical measurements are made in a cell in which a bored-out cone of polytetrafluoroethylene is pressed down against the sample. The bore defines the electrode area (0.70 cm^2). The electrolyte (1 M $HClO_4$), the counter electrode (platinum gauze), and the reference electrode (Ag/AgCl/saturated KCl) are then placed in the bore. Oxygen is not excluded from the cell. A PAR 273 potentiostat, interfaced to a personal computer and modified as described previously to provide smooth potential ramps,[23] is used to record cyclic voltammograms.

Results

Coadsorption of Ferrocene-Terminated Thiols and Unsubstituted Thiols. Figure 2 shows cyclic voltammograms in 1 M $HClO_4$ of mixed monolayers of $FcCO_2(CH_2)_{11}SH$ (Fc = $(\eta^5\text{-}C_5H_5)Fe(\eta^5\text{-}C_5H_4)$) and $CH_3(CH_2)_9SH$ on gold formed in ethanol solutions containing various mole fractions (x_{Fc}) of the ferrocene-terminated thiol. The electrode potential was scanned from the lower limit to the higher limit and back at 100 mV/s, and the current to the electrode was recorded. The shape of the features in the cyclic voltammograms are independent of scan rate from 1 to 100 mV/s, and the height of the peaks scales linearly with scan rate. Repeated scanning does not change the voltammograms, demonstrating that these monolayers are stable to electrochemical cycling in acidic, aqueous solution.

At low mole fraction ($x_{Fc} \leq 0.25$), the ferrocene oxidation and ferricenium reduction peaks are symmetric with a full width at half maximum (fwhm) of about 90 mV and with no splitting between the oxidation and reduction peaks. This is the behavior expected for noninteracting electroactive groups attached to the surface and in rapid equilibrium with the electrode.[4] The width of the peak is due only to the entropy of mixing in this thermodynamically ideal two-dimensional solution of oxidized and reduced sites. The lack of peak splitting between positive and negative scans at 100 mV/s indicates that the rate of electron transfer is rapid on the time scale of the experiment.

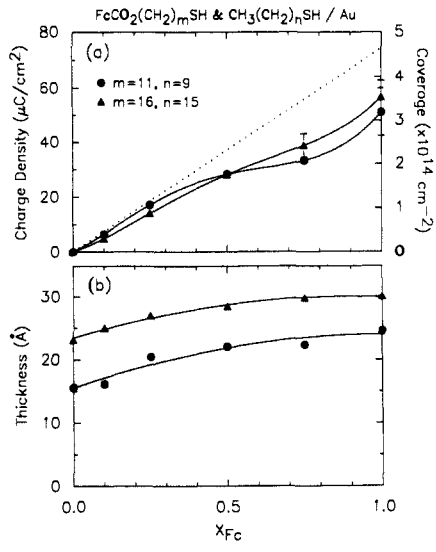

Figure 3. (a) Ferrocene surface charge density and coverage for mixed monolayers of $FcCO_2(CH_2)_{11}SH$ and $CH_3(CH_2)_9SH$ (circles) and $FcCO_2(CH_2)_{16}SH$ and $CH_3(CH_2)_{15}SH$ (triangles) as a function of the mole fraction (x_{Fc}) of the ferrocene-terminated thiol in the adsorption solution. Standard deviation of data is less than the size of the symbols unless indicated. Solid lines are guides to the eye. Dotted line is ferrocene coverage expected for the lattice model shown in Figure 1 with statistical adsorption (see Discussion). (b) Monolayer thickness determined by ellipsometry for the monolayers examined in (a). Solid lines are guides to the eye.

At higher mole fractions of the electroactive thiol in the adsorption solution, the resulting cyclic voltammograms broaden, develop an asymmetry, and finally develop an additional set of peaks as the amount of ferrocene is increased. The breakdown of the thermodynamically ideal behavior of this system as the amount of ferrocene is increased is probably due to a combination of interaction between ferrocene sites and inhomogeneity of those sites at higher surface concentrations.

Increasing the lengths of the chains of both the ferrocene-terminated and the unsubstituted thiols by using $FcCO_2(CH_2)_{16}SH$ and $CH_3(CH_2)_{15}SH$ as coadsorbates results in very similar cyclic voltammograms for x_{Fc} = 0.25, 0.5, 0.75, and 1.0 (not shown). In particular, the anodic and cathodic peaks are not split, and, at the lower coverage, the peaks are symmetric with the ideal width. However, for x_{Fc} = 0.1, the voltammogram, though ideal at 10 mV/s, shows a peak splitting of 27 mV at 100 mV/s. This splitting corresponds to a standard electron-transfer rate constant of 5.2 s^{-1}.[35,36] The lack of a measurable peak splitting at the higher coverages or with the shorter chains indicates that the standard rate constant is greater than about 20 s^{-1} in those cases.[37]

The amount of electroactive ferrocene in the monolayers can be quantitated from cyclic voltammograms such as those in Figure 2. For both the positive and negative scans, a linear background is first subtracted to remove the charging current. The area under the peaks is then integrated and divided by the scan rate to obtain the amount of charge passed to oxidize the ferrocene or reduce the ferricenium sites. The oxidation and reduction charges are the same to within the accuracy of the base line subtraction and are independent of the scan rate from 1 to 100 mV/s. The constancy of charge holds even in those cases where the shape of the features is not independent of scan rate. The surface charge densities (μC/cm^2) obtained by this procedure are converted to

(34) Uchida, I.; Ishiho, A.; Matsue, T.; Itaya, K. *J. Electroanal. Chem.* **1989**, *266*, 455–460.
(35) Standard rate constants are calculated as recommended by Laviron in the quasireversible case assuming $\alpha = {}^1/_2$.[36]
(36) Laviron, E. *J. Electroanal. Chem.* **1979**, *101*, 19–28.
(37) Preliminary AC impedance measurements give standard rate constants on the order of 5×10^3 s^{-1} for mixed monolayers of $FcCO_2(CH_2)_{11}SH$ and $CH_3(CH_2)_9SH$ with x_{Fc} = 0.25 (Glarum, S.; Bertozzi, C.; Chidsey, C. E. D. Unpublished results).

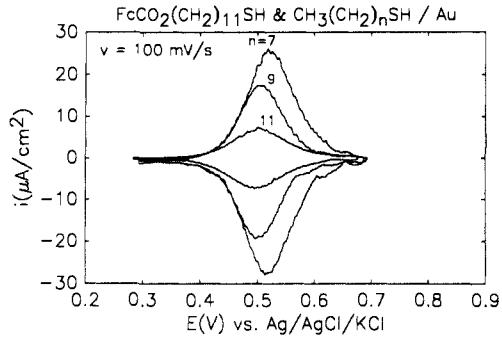

Figure 4. Cyclic voltammograms in 1 M $HClO_4$ of mixed monolayers of $FcCO_2(CH_2)_{11}SH$ and unsubstituted alkanethiols ($CH_3(CH_2)_nSH$) with 7, 9, and 11 methylene units. $x_{Fc} = 0.25$ and scan rate = 100 mV/s.

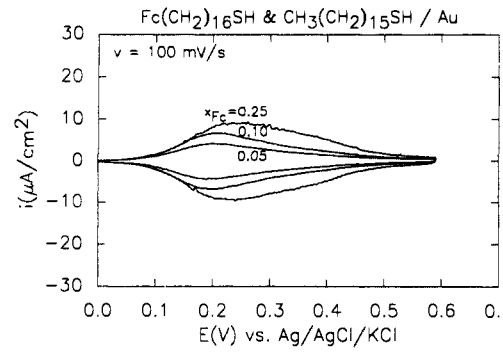

Figure 5. Cyclic voltammograms in 1 M $HClO_4$ of mixed monolayers of $Fc(CH_2)_{16}SH$ and $CH_3(CH_2)_{15}SH$ formed from ethanol solutions containing various mole fractions (x_{Fc}) of the ferrocene-terminated thiol. Scan rate = 100 mV/s.

ferrocene surface coverages by dividing by the electron charge.

Figure 3a shows ferrocene surface charge densities (left axis) and coverages (right axis) plotted vs the mole fraction of the electroactive thiol in the adsorption solution for the two sets of mixed monolayers examined: $FcCO_2(CH_2)_{11}SH$ with $CH_3(CH_2)_9SH$ and $FcCO_2(CH_2)_{16}SH$ with $CH_3(CH_2)_{15}SH$. The amount of ferrocene in the monolayers rises linearly at low mole fraction, then rises more slowly at intermediate compositions, and finally rises again at $x_{Fc} = 1$ (when there is only ferrocene-terminated thiol in the adsorption solution).

The amount of the coadsorbed *n*-alkanethiol in the monolayers cannot be as readily quantitated as can the amount of the ferrocene-terminated thiols. However, ellipsometry provides a check that the total amount of material on the surface is reasonable. Figure 3b shows the thickness of the two sets of mixed monolayers determined by ellipsometry.[38] The lengths of the individual adsorbates, as measured from space-filling molecular models, are 16.8 Å for $CH_3(CH_2)_9SH$, 25.4 Å for $FcCO_2(CH_2)_{11}SH$, 24.4 Å for $CH_3(CH_2)_{15}SH$, and 31.8 Å for $FcCO_2(CH_2)_{16}SH$. As expected, the ellipsometric data show that the thicknesses of the monolayers increases monotonically from about the length of the unsubstituted thiol to about the length of the ferrocene-terminated thiol as the coverage of the ferrocene-terminated thiol is increased.

Role of Chain Length. Figure 3a shows that increasing the length of the chains in *both* the ferrocene-terminated thiol and the unsubstituted thiol does not drastically affect the ferrocene surface coverage. Figure 4 illustrates the importance of the *relative* chain length of the two coadsorbates in determining the composition of the monolayers. At constant mole fraction of ferrocene-terminated thiol in the adsorption solution, the heights and areas of the ferrocene peaks decrease as the chain length of the unsubstituted thiol increases from 7 to 11 methylene groups. The longer the unsubstituted thiol, the lower the coverage of ferrocene-terminated thiol in the monolayer. This trend is similar to effects seen in other mixed monolayer systems without electroactive groups and can, at least in part, be explained by the relative solubilities of the coadsorbates in the ethanol adsorption solutions.[25] Longer alkanethiols are less soluble in ethanol, so their free energies in solution are higher, and their affinity for adsorption (a state more like the solid) should be larger.

In fact, this trend can also be seen in Figure 3a. The lower initial slope of the charge density vs mole fraction for the 16-carbon chain ferrocene-terminated thiol compared with the 11-carbon chain ferrocene-terminated thiol appears to be due to the relative lengths of the coadsorbates in the two cases. In the first case, the unsubstituted thiol has the same number of carbons as the polymethylene chain of the ferrocene-terminated thiol. In the second case, the unsubstituted thiol has one fewer carbon atoms.

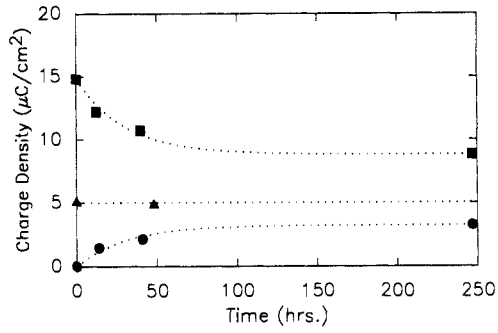

Figure 6. Ferrocene surface charge density of mixed monolayers of $FcCO_2(CH_2)_{16}SH$ and $CH_3(CH_2)_{15}SH$ initially formed in one solution and then exchanged for various times in a second solution. Mole fraction of ferrocene-terminated thiol in first and second solutions: $x_{Fc,1} = 0.25$, $x_{Fc,2} = 0.0$ (squares); $x_{Fc,1} = x_{Fc,2} = 0.1$ (triangles); $x_{Fc,1} = 0.0$, $x_{Fc,2} = 0.25$ (circles). Dotted lines are guides to the eye.

Nonpolar Ferrocene-Terminated Thiols. An important feature of the ferrocene-terminated thiols is the way in which the ferrocene group is attached to the polymethylene chain. Figure 5 shows cyclic voltammograms of mixed monolayers incorporating a ferrocene-terminated thiol in which the ferrocene is attached directly to the polymethylene chain without a polar ester group. A shorter, homologous ferrocene-terminated thiol, $Fc(CH_2)_{11}SH$, coadsorbed with $CH_3(CH_2)_9SH$ gave very similar voltammograms (not shown). Two differences are apparent from a comparison of Figures 2 and 5. First, by replacing the electron-withdrawing ester substituent with an electron-donating alkyl substituent, the oxidation potential of the ferrocene group is shifted negative about 300 mV. The second, and more significant difference, is that the ferrocene peaks in Figure 5 are very broad and asymmetric, with long tails to positive potential, even at the lowest mole fraction examined ($x_{Fc} = 0.05$). The peaks are similar in shape to the peaks for the polar ferrocene-terminated thiols at high mole fractions. This is the case even though the surface charge densities are only about a factor of two higher than for the polar ferrocene-terminated thiols at the same mole fraction and are within the range of charge densities where thermodynamically ideal peak shapes are observed in Figure 2. This highly nonideal behavior at low surface coverage suggests a strong interaction between the nonpolar ferrocene groups, perhaps due to aggregation. This nonideality also seriously complicates the study of electron-transfer kinetics and argues against the directly linked, nonpolar ferrocene-terminated thiols as good systems with which to study electron transfer.

Adsorbate Exchange. Returning to the better-behaved polar ferrocene-terminated thiols ($FcCO_2(CH_2)_nSH$), we examine the effects of taking a supposedly fully equilibrated monolayer out of one adsorption solution and incubating it for various times in another adsorption solution. Similar experiments, without electroactive groups, have been described by Allara and Nuzzo[28] and Whitesides and co-workers.[25a] In one extreme, if thiols equilibrate

(38) Ellipsometry was performed as described elsewhere[23] by using a film refractive index of 1.45. Though not the correct value for the ferrocene group, this refractive index is appropriate for the unsubstituted thiols and allows a qualitative measure of the relative thicknesses of the films.

(39) (a) Morisaki, H.; Ono, H.; Yazawa, K. *J. Electrochem. Soc.* **1988**, *135*, 381–383. (b) Morisaki, H.; Ono, H.; Yazawa, K. *J. Electrochem. Soc.* **1989**, *136*, 1710–1714.

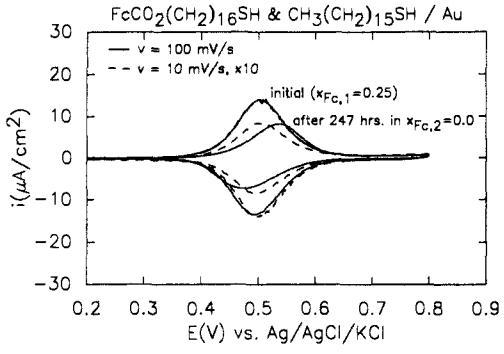

Figure 7. Cyclic voltammograms in 1 M $HClO_4$ of a mixed monolayer of $FcCO_2(CH_2)_{16}SH$ and $CH_3(CH_2)_{15}SH$ ($x_{Fc,1} = 0.25$) before and after incubation for 247 h in a solution of the unsubstituted thiol ($x_{Fc,2} = 0.0$). Scan rates = 100 mV/s (solid) and 10 mV/s (dashed, ×10).

rapidly between the monolayer and an ethanol solution, the monolayer will rapidly come to have the properties of a monolayer formed from clean gold in the new solution. At the other extreme, if the adsorbates adsorb irreversibly when clean gold is first exposed to an adsorption solution, equilibration with later solutions will be impossible.

Figure 6 shows ferrocene surface charge densities as a function of time for three experiments. In the first (squares), a mixed monolayer was first formed by incubating clean gold for 2 days in an ethanol solution of 0.25 mM $FcCO_2(CH_2)_{16}SH$ and 0.75 mM $CH_3(CH_2)_{15}SH$. This monolayer was then incubated in a solution of 1.0 mM $CH_3(CH_2)_{15}SH$. At various times, the sample was removed, rinsed sequentially with ethanol, hexane, ethanol, and water, examined by cyclic voltammetry, and returned to the second adsorption solution. In the complementary experiment (circles), the order of the solutions was switched so that the initial monolayer contained no ferrocene-terminated thiol. In the control experiment (triangles), a monolayer was incubated in only one adsorption solution (of intermediate composition) to check for a change in coverage with time in a single solution.

Figure 6 shows that after changing the solution composition, the composition of the monolayers slowly changes toward that obtained with a bare gold surface in the second solution. However, even after 10 days, the equilibration is not complete. Neither of the films in the two complementary experiments reached the compositions obtained with bare gold. The equilibration process is clearly multiphasic. There is a significant change in the first few hours, but about one quarter of the way to the expected equilibrium charge density the process slows down. It appears there is a portion of the monolayer that exchanges in a day or so, and a large portion that exchanges much more slowly or not at all.

The replacement of some of the ferrocene-terminated thiols with unsubstituted thiols in the first exchange experiment described above had a pronounced effect on the shape of the peaks in the cyclic voltammograms as well as the area under the peaks. The longer the incubation in the ferrocene-free solution, the greater the splitting between the oxidation and reduction peaks. Figure 7 shows the peaks at two scan rates before incubation in the unsubstituted thiol solution and after 10 days in that solution. While there is no peak splitting before exchange and the shape of the voltammograms is independent of scan rate (indicating rapid electron transfer), after a long incubation, a scan rate-dependent peak splitting develops. At 100 mV/s the splitting is 66 mV, giving a standard rate constant of 1.8 s^{-1}.[35,36]

The peak splitting seen when some ferrocene-terminated thiols are replaced with unsubstituted thiols in *not* observed in the complementary experiment in which unsubstituted thiols are replaced with ferrocene-terminated thiols. Furthermore, as noted earlier, a small peak splitting (27 mV at 100 mV/s) *is* observed in monolayers formed in a single solution with a very low mole fraction of ferrocene-terminated thiol ($x_{Fc} = 0.1$). No splitting is observed at 100 mV/s for the higher mole fractions or for the shorter, 11-carbon chain homolog.

Discussion

Our goal is to develop a monolayer system in which the fundamental steps in electron transfer between a metal electrode and a molecular electroactive site can be carefully examined. The model we have in mind for such an assembly is illustrated in Figure 1. Two basic features are needed of a monolayer system for such studies: stability in an electrochemical environment and the ability to systematically change the structure. The data discussed above clearly show that monolayers formed by the coadsorption of ferrocene-terminated thiols with unsubstituted thiols are stable and can be oxidized and rereduced without changing the properties of the monolayer. The surface coverage of the ferrocene-terminated thiols can be adjusted by changing the mole fraction of ferrocene-terminated thiol in the adsorption solution, and the thickness of the layer can be changed by changing the lengths of the chains of the two coadsorbates. Further, the adsorption affinity of the two components from ethanol can be adjusted by the choice of relative chain lengths and the polarity of the particular ferrocene group used.

Beyond these basic features, an important criterion for straightforward determination of electron-transfer kinetics is the independence of each site so that the electrochemistry is that of an ensemble of identical, isolated sites. At low coverages, the ferrocene-terminated thiols containing the polar ester linking group satisfy this criterion. The nonpolar ferrocene-terminated thiols in which the ferrocene is linked directly to the alkane chain clearly do not have identical, independent electroactive sites, even at low coverages, as shown by their nonideal electrochemistry. We currently favor the polar ester linkage, but other linkages, including the direct, nonpolar linkage, may be useful with other adsorption conditions or in other electrochemical environments.

The measurement of ferrocene surface charge density in Figure 3a allows us to quantitate the ferrocene coverage and compare it with simple expectations. The dotted line in Figure 3a is a plot of the coverage expected for the model shown in Figure 1 if the adsorption of the electroactive and electroinactive coadsorbates is purely statistical. In that case, the ferrocene coverage is linearly related to x_{Fc} and, at $x_{Fc} = 1.0$, is taken to be the lattice site density for the $\sqrt{3} \times \sqrt{3}$ R30° lattice on Au (111), 4.64×10^{14} cm^{-2}. At low mole fraction, we find that the statistical model is approximately correct. Deviations from it are probably mostly due to differences in the solvation of the adsorbates in the adsorption solution. This rough agreement, like the thermodynamically ideal electrochemistry, gives us confidence that, at low ferrocene coverage, the actual monolayers of the polar ferrocene-terminated thiols consist of independent ferrocene groups that do not exert a strong influence on the structure of the monolayer.

As an aside, the statistical model *must* be wrong at high coverage because ferrocene groups cannot pack as densely as polymethylene chains. From the diameter of the ferrocene groups used in Figure 1 (6.6 Å[32,33]), the maximum coverage would be 2.7×10^{14} cm^{-2}. In fact, that is about the coverage of ferrocene-terminated thiol at $x_{Fc} = 0.75$ in Figure 3a. At $x_{Fc} = 1$ (in the absence of unsubstituted thiols to act as diluents), the coverage is higher than 2.7×10^{14} cm^{-2}, possibly reflecting the presence of some ferrocene groups folded in among the poorly packed polymethylene chains.

Another important criterion for the applicability of these monolayers to the study of electron transfer is the rigidity of the lattice of packed polymethylene chains. Rigidity is needed to hold the ferrocene groups away from the surface and also to prevent them from diffusing to the inevitable defect sites in the monolayer. By using the electroactivity of the ferrocene group as a convenient probe, we have shown that most of the adsorbates in these monolayers do not exchange readily with adsorbates in solution (Figure 6). This exchange experiment is important evidence of the robust quality of these monolayers.

The data suggest that a small fraction of the thiols are relatively easily exchanged and that the rest are only *very slowly exchanged if at all.* A model to explain this behavior is suggested by the results of diffraction experiments on the unsubstituted alkanethiol monolayers. Though diffraction of both electrons[24] and helium

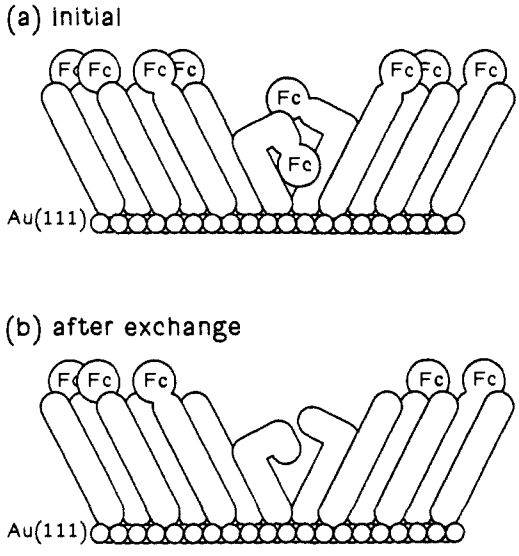

Figure 8. Cartoons depicting the structure of a domain boundary in a mixed monolayer of ferrocene-terminated and unsubstituted alkanethiols on Au(111) before (a) and after (b) exchange in a solution of the unsubstituted thiol.

atoms[22] has been observed for these monolayers, the broad line shapes and high incoherent scattering suggest that the samples are composed of domains about 50–100 Å across. The easily exchanged fraction of the monolayer may be associated with the domain boundaries and the unexchanged fraction associated with the interior of the domains.

Figure 8 shows a pair of cartoons of a tilt domain boundary and the adjacent domains of the lattice before and after exchange. Before exchange, the ferrocene-terminated thiols are shown to be randomly distributed between the domain-boundary region and the interior of the domains. After exchange, the ferrocene-terminated thiols in the region of the domain boundary have been replaced by unsubstituted alkanethiols. We expect exchange of thiols in the interior of the domains to require chains to diffuse from within the densely packed chain region to a domain-boundary region. If the domain-boundary model is correct, then that process is apparently quite slow.

Tilt domain boundaries, as depicted in Figure 8, are not the only candidate for the defective sites. Other possible causes of domain boundaries include step edges, accumulated impurities on the gold surface, and grain boundaries in the gold film. Whatever their origin, it is likely that the boundaries between domains will be highly defective and the sites of rapid exchange of adsorbates relative to the more numerous lattice sites within the domains. The defective sites may be due to inhomogeneities other than domain boundaries. Detailed chemical, structural, and spectroscopic experiments will be needed to identify conclusively the microscopic origin of these defective sites. The important point for the current study is that they can be exchanged thus removing the defective, *electroactive* sites.

From the exchange experiments, it is evident that the monolayers do not necessarily have equilibrium structures.[25a] While a partially formed monolayer may equilibrate with the adsorption solution during the early stages of assembly, the complete monolayer does not equilibrate on the normal laboratory time scale of many days. How can this irreversibility be reconciled with the observed variation of the adsorption affinity with the relative free energy of the adsorbates in solution? One possible mechanism is equilibrium physisorption of the coadsorbates at the surface followed by much less reversible chemisorption and incorporation into the dense monolayer.

The exchange experiments provide a second, quite different demonstration of the structural integrity of the majority of the monolayer structure. Removing a few easily exchanged sites reduces the rate of electron transfer to and from the remaining sites by at least an order of magnitude to a rate that can be measured by voltammetry at 100 mV/s (standard rate constant of 1.8 s^{-1}). This is strong evidence that the majority of the adsorbates in the monolayer are in structurally well-defined environments with the ferrocene groups held away from the surface of the electrode. Only a minority of the sites have disordered packing that allows the ferrocene groups to get close to the electrode. At high enough ferrocene coverage, these defective sites can act as intermediates for electron transfer to the other sites unless they are removed by exchange for electroinactive adsorbates.

Evidence for a defect mediated pathway for electron transfer at high coverage comes from the decrease in the rate of electron transfer in unexchanged monolayers as the ferrocene coverage is lowered. At $x_{Fc} = 0.25$, the monolayer formed from $FcCO_2(CH_2)_{16}SH$ and $CH_3(CH_2)_{15}SH$ has a rate of electron transfer that is too fast to measure by voltammetry at 100 mV/s, but at $x_{Fc} = 0.1$ the rate is low enough to measure (standard rate constant of 5.2 s^{-1}). This coverage dependence implies that electron exchange between ferrocene groups is an important pathway for electron transfer in unexchanged monolayers.

Outlook for Future Studies. The robust and well-defined nature of the self-assembled monolayers formed by coadsorption of ferrocene-terminated and unsubstituted alkanethiols on gold allows numerous valuable experiments to probe the basic aspects of interfacial electron transfer. Detailed kinetic measurements are in progress and will be reported separately. The combination of dilution of electroactive sites and exchange of defective sites offers the best opportunity to date to probe the distance dependence of electron transfer at the electrochemical interface. Another important goal is the measurement of the relationship between the thermodynamic driving force and the activation energy of the electron transfer. In principle, electron transfer at an electrode is ideally suited to examining that relationship because both the temperature and thermodynamic driving force can be readily varied. However, experiments in the crucial range of large driving forces are difficult because the reactions become very rapid. The low rates of electron transfer in the monolayers described here allow that relationship to be examined out to large driving forces. Similar experiments have been conducted with soluble electroactive species at oxide covered electrodes.[39] Finally, the role of the structure and the electronic properties of the material across which an electron transfers has been difficult to explore, but may be accessible with this type of monolayer assembly as the repertoire of the monolayer self-assembly technique expands to include spacers other than alkane chains.

Supplementary Material Available: Details of the adsorbate syntheses and analyses (6 pages). Ordering information is given on any current masthead page.